Cordycepin interferes with 3′ end formation in yeast independently of its potential to terminate RNA chain elongation

SANDRA HOLBEIN,[1,2] AGNIESZKA WENGI,[1] LAURENCE DECOURTY,[3] FLORIAN M. FREIMOSER,[4] ALAIN JACQUIER,[3] and BERNHARD DICHTL[1]

[1]Institute of Molecular Biology, University of Zürich, CH-8057 Zürich, Switzerland
[2]Ph.D. Program in Molecular Life Sciences, University of Zürich and Swiss Federal Institute of Technology (ETH) Zürich, CH-8092 Zürich, Switzerland
[3]Unité de Génétique des Interactions Macromoléculaires, CNRS-URA2171, Institut Pasteur, 75724 Paris CEDEX 15, France
[4]Institute of Plant Sciences, Swiss Federal Institute of Technology (ETH) Zürich, CH-8092 Zürich, Switzerland

ABSTRACT

Cordycepin (3′ deoxyadenosine) is a biologically active compound that, when incorporated during RNA synthesis in vitro, provokes chain termination due to the absence of a 3′ hydroxyl moiety. We were interested in the effects mediated by this drug in vivo and analyzed its impact on RNA metabolism of yeast. Our results support the view that cordycepin-triphosphate (CoTP) is the toxic component that is limiting cell growth through inhibition of RNA synthesis. Unexpectedly, cordycepin treatment modulated 3′ end heterogeneity of *ACT1* and *ASC1* mRNAs and rapidly induced extended transcripts derived from *CYH2* and *NEL025c* loci. Moreover, cordycepin ameliorated the growth defects of poly(A) polymerase mutants and the *pap1-1* mutation neutralized the effects of the drug on gene expression. Our observations are consistent with an epistatic relationship between poly(A) polymerase function and cordycepin action and suggest that a major mode of cordycepin activity reduces 3′ end formation efficiency independently of its potential to terminate RNA chain elongation. Finally, chemical-genetic profiling revealed genome-wide pathways linked to cordycepin activity and identified novel genes involved in poly(A) homeostasis.

Keywords: cordycepin; ATP; poly(A); 3′ end formation; transcription; RNA; *Saccharomyces cerevisiae*

INTRODUCTION

The adenosine analog cordycepin (3′ deoxyadenosine) was first isolated from the ascomycete fungus *Cordyceps militaris* (Cunningham et al. 1950). Due to the absence of a 3′-hydroxyl moiety, the incorporation of cordycepin during RNA synthesis will result in termination of chain elongation. This activity has been well described in vitro with purified RNA polymerases and poly(A) polymerases from a number of organisms including yeast (Horowitz et al. 1976) and mammals (Muller et al. 1977). Furthermore, cordycepin exhibits well-established anti-bacterial, anti-fungal, and anti-parasitic properties (Sugar and McCaffrey 1998; Ahn et al. 2000; Rottenberg et al. 2005). In humans, anti-oxidant, anti-inflammatory, and anti-proliferative activities have been attributed to the drug (Zhu et al. 1998a,b). Indeed, for centuries, the fungus *Cordyceps sinensis* has been a widely administered traditional Chinese medicine, and cordycepin is thought to be one of the bioactive components mediating a host of beneficial effects (Paterson 2008). While the therapeutic potential of cordycepin underscores its unique properties, the effects of the drug on RNA metabolism are not completely understood. However, cordycepin was previously used to screen for novel genes involved in pre-mRNA polyadenylation (Bloch et al. 1978). This identified *RNA14* and *RNA15* genes, which encode core components of the 3′ end formation machinery in yeast (Minvielle-Sebastia et al. 1994). Thus, cordycepin responsive growth phenotypes may be useful indicators to detect deficiencies in pre-mRNA processing.

In this work, we present the first comprehensive analysis of the molecular effects of cordycepin in the budding yeast *Saccharomyces cerevisiae*. We provide evidence that the drug interfered with RNA synthesis and that this effect is

mediated by CoTP, the toxic derivative of cordycepin. Unexpectedly, we observed defects during 3′ end formation of transcripts that occurred independently of a possible role of CoTP in terminating RNA chain elongation. Genome-wide chemical genetic profiling identified mutations that mediated cordycepin-responsive growth and linked novel genes to poly(A) metabolism. Our results extend the understanding of the molecular effects of the drug and establish cordycepin responsive growth as a functional test for the characterization of unknown genes.

RESULTS

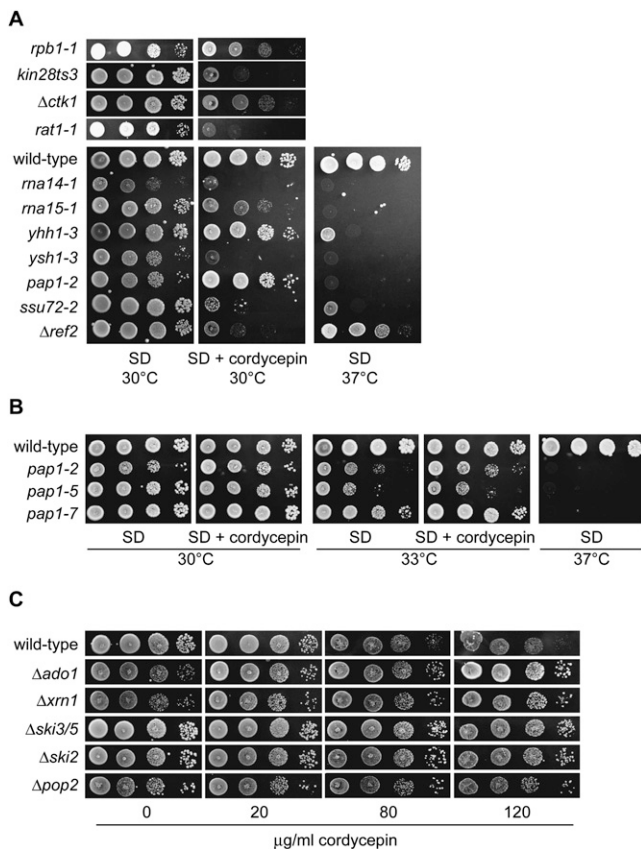### Cordycepin toxicity in yeast is due to the inhibition of RNA synthesis

To analyze the molecular effects of cordycepin, we initially tested mutants in RNA synthesis pathways for hypersensitive growth in the presence of the drug (Fig. 1A). In these experiments, we employed a concentration of 20 μg/mL

FIGURE 1. Cordycepin-responsive mutant yeast strains involved in RNA synthesis and turn-over. (*A–C*) The indicated yeast strains were grown overnight in synthetic complete (SD) medium at the appropriate temperature. Tenfold serial dilutions were produced and spotted on media lacking or containing cordycepin and grown for 3–5 d. Unless indicated otherwise, the cordycepin concentration used was 20 μg/mL.

cordycepin, which only mildly affected growth of a wild-type strain (10% increased doubling time in liquid culture) (data not shown). We observed hypersensitive growth associated with mutants in the largest subunit of RNAP II (*rpb1-1*), kinases that phosphorylate the serine 5 (*kin28-ts3*) and serine 2 residues (*Δctk1*) of the RNAP II carboxy-terminal domain (CTD), a serine 5 CTD phosphatase (*ssu72-2*), and the nuclear 5′–3′ exonuclease Rat1 (*rat1-1*). Furthermore, mutants in certain 3′ end formation components responded strongly to the drug. This included the *rna14-1* and *rna15-1* strains, which were initially identified based on cordycepin sensitivity (Bloch et al. 1978), a mutation in the putative 3′ end nuclease Ysh1/Brr5 (*ysh1-3*), and the 3′ end factor Ref2 (*Δref2*). In contrast, mutation of Yhh1/Cft1 (*yhh1-3*) was without effect, and a mutant in poly(A) polymerase (*pap1-2*) showed increased resistance to cordycepin. To corroborate the latter observation, we tested additional mutant alleles in poly(A) polymerase and found that the *pap1-2* and *pap1-7* mutants reproducibly displayed a distinct growth advantage at 33°C on cordycepin medium (Fig. 1B). With the exception of the paradoxical behavior of *pap1* mutants, cordycepin enhanced the growth defects of mutations in transcription and pre-mRNA 3′ end formation, consistent with a negative impact on RNA synthesis.

While the enhancement of growth defects linked cordycepin activity to RNA metabolism, it is less clear whether inhibition of RNA synthesis is the reason for reduced cell growth. To get a better understanding of cordycepin toxicity, we identified mutations that ameliorated the inhibitory effects of the drug (see below). Consistent with previous results (Lecoq et al. 2001), we found that the absence of the adenosine kinase Ado1 suppressed cordycepin toxicity at high cordycepin concentrations that reduced growth of a wild-type strain (Fig. 1C, 120 μg/mL). Ado1 converts cordycepin to cordycepin-monophosphate (CoMP), which is transformed into cordycepin-triphosphate (CoTP) by adenylate kinase Adk1 (Konrad 1988). Since *Δadk1* cells were also resistant to cordycepin (see below), we conclude that CoTP, rather than cordycepin, is the toxic component. Strikingly, we found that the absence of various components involved in cytoplasmic mRNA turnover also suppressed cordycepin toxicity. This included the 5′–3′ exonuclease Xrn1 (Muhlrad et al. 1994), the Pop2 deadenylase (Daugeron et al. 2001), and Ski2 and Ski3/5 proteins that aid exosome mediated (3′–5′ directed) RNA turn over (Brown et al. 2000). The observation that RNA stabilization suppressed cordycepin toxicity is consistent with the idea that RNA synthesis is limiting cell growth in the presence of the drug.
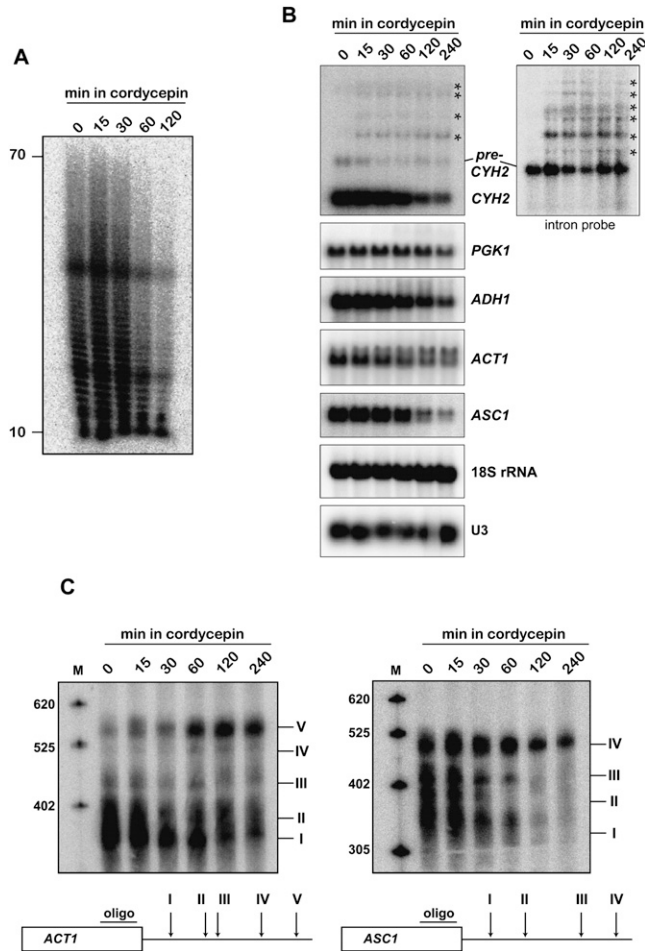
Effects of cordycepin on mRNA synthesis in wild-type strains

Next, we exposed wild-type strains to 20 μg/mL cordycepin and performed RNA analyses. Cellular poly(A) content was

strongly reduced after 2 h, consistent with a strong inhibition of RNA synthesis (Fig. 2A). Probing of individual housekeeping mRNAs by Northern blot revealed reduced steady-state levels for *CYH2*, *ASC1*, and *ADH1* and a less
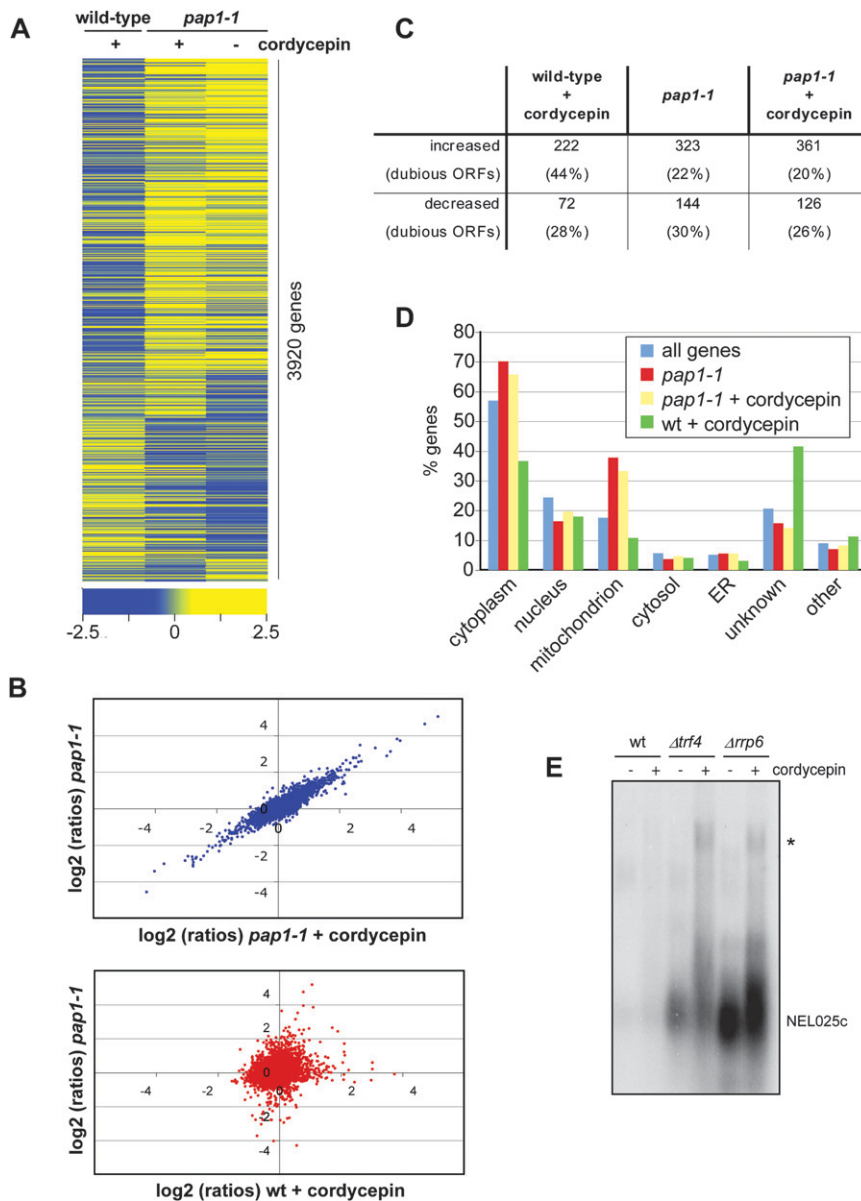
severe effect on *ACT1* and the stable *PGK1* mRNA (Fig. 2B); levels of 18S rRNA, U3 snoRNA, and $tRNA_3^{LEU}$ remained unchanged (Fig. 2B; data not shown). Most interestingly, we observed additional, longer RNAs for *CYH2*, which appeared as early as 15 min after cordycepin addition. These RNAs extended more than 3 kb beyond the normal 3′ end of the mRNA. Furthermore, a probe directed against the *CYH2* intron readily detected the pre-mRNA and extended transcripts (Fig. 2B).

Moreover, we observed a pattern of *ACT1* mRNA in the presence of cordycepin that was reminiscent of poly(A) site selection defects previously associated with mutants in the 3′ end formation machinery (Mandart and Parker 1995; Dichtl et al. 2002b; Kyburz et al. 2003). To analyze the 3′ ends of *ACT1* , we targeted the RNA with an oligonucleotide directed against the open reading frame (ORF) and RNase H (Fig. 2C). This resulted in 5′ truncation of the mRNA and allowed the size separation on high-resolution gels of transcripts with at least five different 3′ ends (Dichtl et al. 2002b). In the absence of cordycepin site I was used predominately, but addition of the drug triggered the disappearance of this species and the accumulation of longer transcripts, which mostly use site V. Notably, this effect was not observed with Δ*ado1* cells (data not shown), suggesting that CoTP may be the active compound mediating this effect. Interestingly, a similar phenotype was observed with *ASC1* mRNA. This transcript also displayed heterogeneous 3′ ends in wild-type strains, and we could resolve at least four different RNA species following RNase H treatment as described above (Fig. 2C). In the absence of cordycepin the different transcripts were roughly equal in abundance, but addition of the drug resulted in exclusive usage of the most distal 3′ end after 2 h. These results suggested that cordycepin reduced the efficiency of 3′ end formation at a step prior to poly(A) tail synthesis by poly(A) polymerase.

The *pap1-1* mutation neutralizes the effects of cordycepin on gene expression

Our results indicated complex effects of cordycepin on RNA metabolism of yeast, and we were intrigued by its mitigating effects on growth of poly(A) polymerase mutants. To extend our experiments, we determined by microarray analyses changes in RNA levels that were induced within 1 h by 20 μg/mL cordycepin in wild-type and *pap1-1* strains. The obtained data, depicted as a heat map in Figure 3A and as a scatter plot in Figure 3B, revealed a high correlation of signals obtained with the *pap1-1* strain in the absence or presence of the drug, respectively. This suggested that the *pap1-1* mutation largely neutralized the negative effects of cordycepin on gene expression. In contrast, the effects of cordycepin treatment of wild-type and the effects of the *pap1-1* mutation were not correlated (Fig. 3A,B), suggesting that the two conditions had distinct effects on RNA levels.

FIGURE 2. Molecular effects of cordycepin on RNA metabolism. (*A*) Cellular poly(A) length distribution following cordycepin treatment. Total RNA was extracted from wild-type strains following growth in the presence of 20 μg/mL cordycepin for the indicated times. RNAs were labeled with [α-^{32}P]cordycepin and poly(A) polymerase, and digested with RNases A and T1. RNase-resistant poly(A) tails were resolved on denaturing 15% polyacrylamide/8.3 M urea gels and visualized by PhosphorImaging (Fuji FLA7000). (*B*) Northern analysis of RNA obtained from a wild-type strain treated with cordycepin as described in *A*. RNAs were detected with random prime labeled probes directed against the open reading frames (ORF) of the indicated genes; (*left* panel) the probes against *CYH2* were either directed against the entire ORF or (*right* panel) exclusively against its intron. (Asterisks) 3′-Extended transcripts. 18S rRNA and U3 snoRNA were detected with end-labeled oligonucleotides. (*C*) High-resolution Northern analysis of *ACT1* and *ASC1* 3′ ends. Total RNA from a wild-type strain treated with cordycepin as described in *A* was treated with RNase H in the presence of oligonucleotides complementary to the 3′ end of the ORF of the (*left* panel) *ACT1* or (*right* panel) *ASC1* genes, respectively. *Below* each gel a scheme indicates the relative location of the oligonucleotide used to target RNAse H and the distribution of observed 3′ ends (I to V for *ACT1*; and I to IV for *ASC1*).

A Heat map — 3920 genes; color scale: -2.5 , 0 , 2.5

B Scatterplots

log2 (ratios) pap1-1 (y-axis) vs log2 (ratios) pap1-1 + cordycepin (x-axis)

log2 (ratios) pap1-1 (y-axis) vs log2 (ratios) wt + cordycepin (x-axis)

C

	wild-type + cordycepin	pap1-1	pap1-1 + cordycepin
increased	222	323	361
(dubious ORFs)	(44%)	(22%)	(20%)
decreased	72	144	126
(dubious ORFs)	(28%)	(30%)	(26%)

D % genes bar chart (legend: all genes, pap1-1, pap1-1 + cordycepin, wt + cordycepin) across categories: cytoplasm, nucleus, mitochondrion, cytosol, ER, unknown, other

**E** Northern blot: wt, Δtrf4, Δrrp6 (− / + cordycepin); * ; NEL025c

FIGURE 3. The *pap1-1* mutation neutralizes the effects of cordycepin. Gene expression profiling was done with wild-type and *pap1-1* strains following a shift for 1 h to medium lacking or containing 20 μg/mL cordycepin, respectively. All experiments were performed in triplicate. (*A*) Heat map of gene expression changes of cordycepin treated wild-type and nontreated and treated *pap1-1* mutant strains relative to the untreated wild-type control. Rows represent genes, and columns represent average values obtained from three independent measurements for the indicated condition; only those 3920 features were represented that gave three values each for all three conditions. Clustering was done with Spearman Row correlation (substance and row) using Acuity 4.0. The color code indicates the distribution of log$_2$ ratios. (*B*) Scatterplot of gene expression changes (log$_2$ ratios). (*Upper* graph) Plots signals obtained with the *pap1-1* strain in the absence (*y*-axis) and the presence (*x*-axis) of cordycepin. (*Lower* graph) Signals obtained with the *pap1-1* strain in the absence of cordycepin (*y*-axis) are plotted against signals obtained with cordycepin-treated wild-type (*x*-axis). (*C*) The table displays the numbers of RNA transcripts that changed at least twofold (log$_2$ value ±1) relative to untreated wild type in the respective conditions. The numbers of transcripts that were derived from dubious open reading frames are indicated in percent in brackets. (*D*) Transcripts that were increased under the indicated conditions were subjected to Gene Ontology analysis using the SGD slim mapper (http://www.yeastgenome.org/). The number of genes in the individual compartments is presented in percent of all analyzed genes. Also indicated is the background distribution of all genes. (*E*) Northern blot analysis of total RNA obtained from wild-type and mutant strains following growth in the absence and presence of 20 μg/mL cordycepin. The CUT *NEL025c* was detected using a random primed labeled probe. (Asterisk) Indicates a transcript that accumulates due to Pap1 dependent 3′ end formation at a downstream gene (Wyers et al. 2005).

Moreover, the microarray data suggested that cordycepin treatment of the wild type resulted in more transcripts that were increased rather than decreased (Fig. 3C). This was surprising since we observed a loss of cellular poly(A) associated with cordycepin treatment (Fig. 2A). These observations may indicate that global levels of transcript bodies (which were detected in the microarray) and of poly(A) tails [which were detected in the poly(A) analysis] were differentially affected by the drug. Interestingly, RNAs derived from dubious open reading frames (dubious ORFs) were over-represented in the category of increased transcripts (Fig. 3C, 44%). A Gene Ontology (GO) analysis revealed, furthermore, that cytoplasmic components were decreased and unknown components were approximately twofold increased under this condition (Fig. 3D). Unknown components are largely constituted by dubious ORFs that also include cryptic unstable transcripts (CUTs) (Wyers et al. 2005). CUTs are rapidly degraded by the nuclear exosome in a reaction that is strongly stimulated by the noncanonical TRAMP poly(A) polymerase complex (Wyers et al. 2005; Houseley et al. 2006). To test whether cordycepin interfered with this pathway, we probed by Northern blot for the abundance of the well-characterized CUT *NEL025c* in wild-type, exosome (Δ*rrp6*), and TRAMP (Δ*trf4*) mutant strains. The CUT was barely detectable in wild type (Fig. 3E). In contrast, *NEL025c* was stabilized in Δ*rrp6* and Δ*trf4* strains, as expected, and cordycepin enhanced this effect, resulting in a striking accumulation of extended transcripts. Taken together, these observations are consistent with the idea that the increase of transcript levels following cordycepin treatment can partially be explained by elevated levels of CUTs and extended CUT containing RNAs.

Most interestingly, we observed a highly significant up-regulation of ATP synthesis pathways in *pap1-1* strains including, among others, mRNAs encoding proteins involved in nucleotide precursor generation (*P*-value = 2.69 E-35), mitochondrial electron transport (*P*-value = 3.17 E-25), and oxidative

phosphorylation (P-value = 1.43 E-40). Moreover, mitochondrial components were strongly over-represented in the GO term analysis (Fig. 3D). This may indicate that less effective Pap1 stimulated the cell to increase ATP production, suggesting that the *pap1-1* mutant had an increased ratio of ATP/CoTP in the presence of cordycepin. Since this ratio may determine cordycepin toxicity (see above), enhanced ATP synthesis may underlie the observed cordycepin resistance of *pap1* mutants. To further test this idea, we supplemented cordycepin-containing medium with adenine. Adenine was used instead of ATP because yeast do not have an adenosine transporter (Maser et al. 1999). Figure 4A shows that excess adenine was sufficient to suppress the growth-inhibitory effect of the drug on a wild-type strain, whereas growth of *pap1* mutant strains was not noticeably affected.

Measurement of the cellular ATP content revealed significantly increased levels in *pap1-2* and *pap1-5* strains at 25°C compared to wild type (Fig. 4B). Following growth at semipermissive temperature (33°C), all tested mutant strains displayed markedly (two- to fourfold) increased ATP levels compared to the wild-type control. These data support the conclusion that ATP levels were elevated in response to less active poly(A) polymerase in the tested temperature-sensitive mutants.
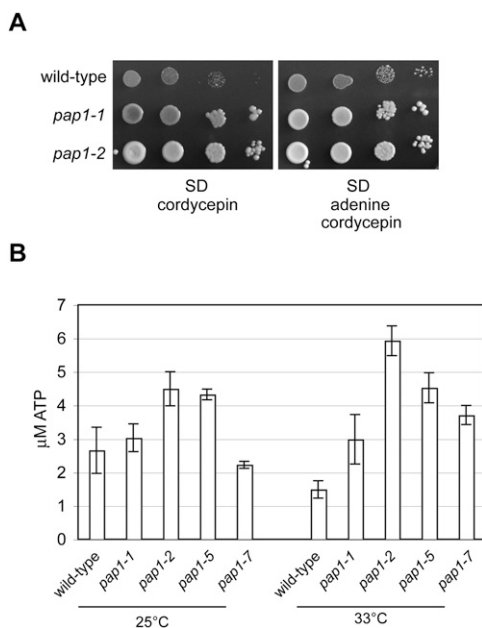

FIGURE 4. Increased ATP levels in *pap1* mutants. (*A*) Tenfold serial dilutions of wild-type and *pap1* mutant strains were spotted on SD medium containing 20 μg/mL cordycepin that was supplemented with 20 μg/mL adenine as indicated. The yeast were grown for 3 d at 25°C and photographed. (*B*) Wild-type and *pap1* mutants strains were grown at 25°C or shifted for 1 h to 33°C as indicated and assayed for ATP content. Represented in the graph are average values for ATP content obtained from three independent yeast cultures; the error bars display standard error.

Genome-wide identification of cordycepin targets

The yeast gene deletion collection (Winzeler et al. 1999) is a valuable tool to explore the molecular targets of therapeutic agents and xenobiotics (Hillenmeyer et al. 2008). To identify mutants that displayed cordycepin-dependent growth phenotypes, we tested more than 4800 haploid deletion strains by spotting them as single drops on synthetic minimal plates lacking or containing 20 μg/mL cordycepin. Candidate strains were identified by visual inspection and re-examined in two consecutive rounds by dropping 10-fold serial dilutions on plates containing 40 and 20 μg/mL cordycepin, respectively. This identified 155 sensitive strains and five strains that showed increased resistance (see also Fig. 1C). The mutants were categorized as strong (57), medium (56), and weak (47) indicating the severity of the growth difference and the relative confidence in the observed phenotype. Figure 5A shows growth phenotypes of selected strains, a full list of identified mutants is supplied in Supplemental Data S1. The distribution of GO components revealed that cordycepin targets were distributed without bias in the individual cellular compartments. Significant functional categories included ATPases (P-value = 0.001) and chromatin binding (P-value = 0.003). Several subunits of the transcriptional coactivator SAGA (Spt3, Spt7, Spt8, and Spt20), the SWR1 chromatin remodeling ATPase, and its substrate, the H2A variant Htz1, were found to be cordycepin-responsive.

A limitation of evaluating drug-dependent growth by drop-test is that weak differences are difficult to detect. We decided therefore to employ a quantitative approach to measure the relative fitness of mutant strains in the absence and presence of the drug by chemical-genetic profiling (Ooi et al. 2006). In these experiments, all mutants of the deletion collection were competitively grown in a single culture, and the relative abundance of individual strains was measured after zero, 12, and 18 generations in medium lacking or containing 20 μg/mL cordycepin. Considering only signals of at least twofold or higher, we identified 205 cordycepin responsive mutants after 12 generations and 496 mutants after 18 generations (complete data sets are available in Supplemental Data S2). However, due to severe growth defects, this procedure will not resolve signals for around 300 to 400 strains (Decourty et al. 2008). The strong increase of identified strains from 12 to 18 generations suggested that even small growth differences could be resolved with this approach. The scatterplot shown in Figure 5B revealed a strong correlation of signals obtained after 12 and 18 generations, demonstrating that the smaller data set was almost completely included in the larger one underscoring the significance of the obtained results.

We could identify several groups of genes that were significantly enriched and that are highlighted in Figure 5B. This included 15 *PEX* genes (P-value = 2.42 E-10), which are required for the biogenesis and proliferation of
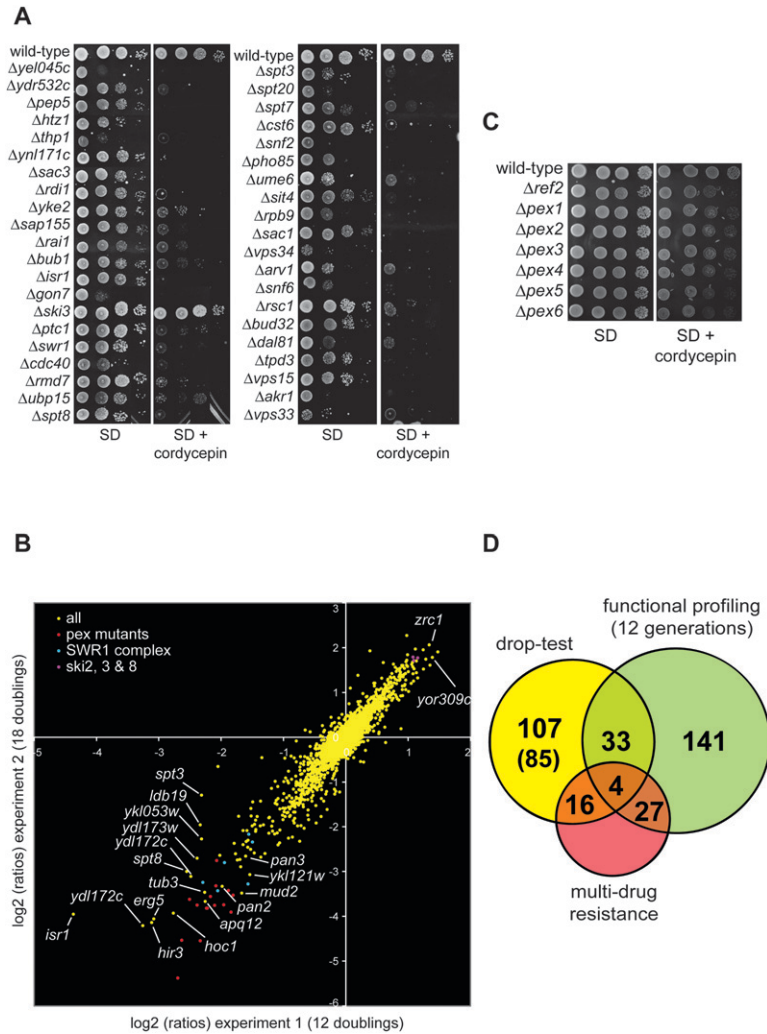
FIGURE 5. Identification of cordycepin-responsive haploid deletion mutants. (*A*) The growth phenotypes of strains identified by drop-test screening were analyzed on medium containing or lacking 40 µg/mL cordycepin as indicated. Strains were grown for 3 d at 30°C and photographed. (*B*) Pools of all viable haploid deletion mutants from the systematic deletion library were grown in complete liquid medium with or without 20 µg/mL cordycepin for 12 or 18 generations (Experiments 1 and 2, respectively) by serial dilutions. Cells were then collected, the genomic DNA was extracted, and the barcode sequence tags associated with each gene deletion were amplified by PCR and hybridized on barcode DNA arrays as described (Decourty et al. 2008). The figure plots for each experiment (Experiment 1 on the *x*-axis and Experiment 2 on the *y*-axis) the log$_2$ of the ratio for each deletion mutant of the barcode signal between the cultures without and with cordycepin (computed as in Decourty et al. 2008). Negative log$_2$ (ratios) indicate strains more sensitive to cordycepin than the average population of mutants. Mutants in *PEX* genes, SWR1 complex genes, and *SKI 2*, *3*, and *8* genes are color-coded as indicated. Arrows and labels point to mutants with strong phenotypes. (*C*) Cordycepin-sensitive growth phenotypes of *pex* mutants. The indicated strains were analyzed as described in *A*. (*D*) Graph depicting the overlap of mutants identified in drop-test screening versus functional profiling (after 12 generations). Also indicated are the numbers of multi-drug-resistance genes that were identified with the individual procedures or which are shared, respectively. In brackets the number of strains are indicated that are identified in the drop-test screening that could not be analyzed by functional profiling due to slow growth of the mutants.

peroxisomes (Kiel et al. 2006). Since cordycepin caused reduced growth of *pex* mutants (Fig. 5C; data not shown), we suggest a role for these organelles in suppressing toxicity of the drug. Interestingly, the catabolism of purines was

associated with peroxisomes in mammals (Wanders and Waterham 2006). If this holds true also for yeast, cordycepin levels may be increased in *pex* mutants due to decreased nucleotide turn-over providing a plausible explanation for the increased sensitivity to the drug.

Most interestingly, chromatin remodeling complexes (*P*-value = 1.03 E-06) and the SWR1 complex (*P*-value = 8.90 E-07) were significantly enriched in these profiling experiments, and the same GO terms were also identified with the drop-test procedure. Similarly, the cordycepin-sensitive growth of mutants lacking SAGA components Spt3 and Spt8 was reproduced in both approaches. We were surprised to identify in this screen strains lacking the Pan2 and Pan3 proteins as cordycepin-sensitive. Pan2/3 form the Pab1p-dependent poly(A) nuclease that acts in the shortening of mRNA poly(A) tails (Boeck et al. 1996; Brown et al. 1996) and that may act in the message-specific maturation of poly(A) length (Brown and Sachs 1998). In contrast, we found that the absence of Pop2, which is associated with the major yeast deadenylase Ccr4 (Daugeron et al. 2001; Tucker et al. 2002), suppressed cordycepin toxicity (Fig. 1C). Thus, these cordycepin-dependent phenotypes may reflect partially antagonistic effects of Pan2/3 and Ccr4/Pop2 deadenylase complexes, respectively, on gene expression in yeast.
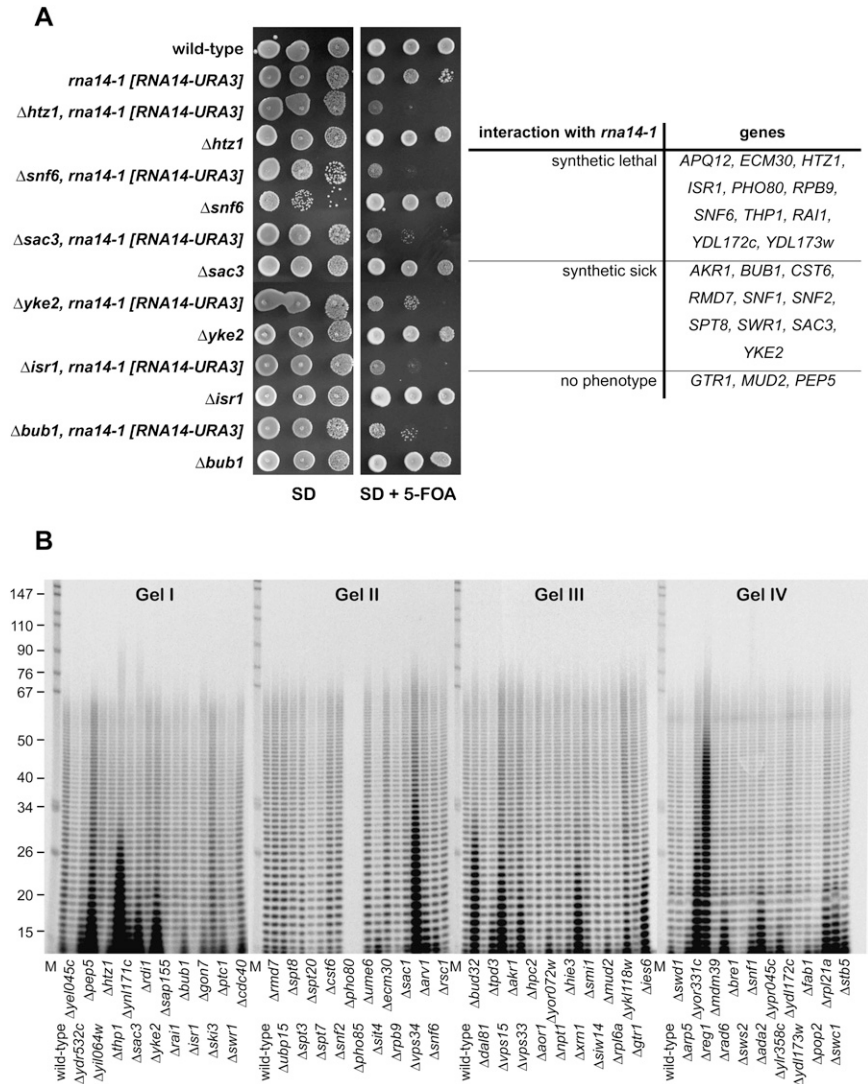
Finally, we compared the results obtained with the drop-test and functional profiling approaches, respectively. Figure 5D shows that a mere 37 mutant strains were identified with both procedures. Since only four of those overlapping mutants corresponded to multi-drug-resistance genes (Parsons et al. 2006), this group of mutants appeared particularly responsive to cordycepin. The limited overlap is mainly due to fact that a large fraction of mutants identified in the drop-test (85 of 107 strains) escaped the analysis by functional profiling due to the slow growth phenotype. Interestingly, we found that a published drop-test screen with mycophenolic acid (Desmoucelles et al. 2002) also overlapped only little with results of a profiling experiment that

we performed with the same drug (S. Holbein, L. Decourty, A. Jacquier, and B. Dichtl, unpubl.). These observations indicate that the outcomes of drug-sensitivity screening of the yeast deletion collection may be strongly dependent on the employed approach.

Cordycepin-responsive strains are connected to poly(A) metabolism

Since pre-mRNA 3′ end formation is targeted by cordycepin, drug mediated growth phenotypes may indicate a functional link to poly(A) metabolism. We therefore tested whether cordycepin-induced growth phenotypes can be duplicated by combining selected mutations with the temperature-sensitive *rna14-1* allele, which is defective in cleavage and polyadenylation of pre-mRNA (Minvielle-Sebastia et al. 1994). Out of 24 double mutants tested, 11 were synthetic lethal, 10 were synthetic sick, and three did not exhibit a phenotype (Fig. 6A). These results suggested a functional association of cordycepin-responsive mutants and pre-mRNA processing.

To corroborate these findings, we asked whether poly(A) metabolism was affected in cordycepin-responsive strains and analyzed the cellular poly(A) length distribution of selected mutants. Figure 6B shows that wild-type strains exhibited an even distribution of poly(A) ranging from about 10 to 70 adenylate residues (As). While the majority of tested strains were similar to wild type, some mutants showed marked accumulation of short (up to 20 As), intermediate (up to 35 As), and long (up to 50 As) A-tracts. The maximum poly(A) length of most strains was within the expected range of ∼70 As. However, Δ*thp1* and Δ*sac3* mutants (Gel I) showed some hyperadenylation, a phenotype that was previously associated with defective mRNA export (Hilleren and Parker 2001). Somewhat curiously, Δ*pho85* and Δ*pho80* RNAs did not give any poly(A) labeling (Gel II). We recently showed that polyphosphate levels were elevated in these mutants, resulting in the inhibition of the in vitro labeling reaction and pointing to a possible role for this metabolite in regulating poly(A) polymerase (Holbein et al. 2008). Short poly(A) tails were stabilized, for example, in the Δ*xrn1* strain, that lacks 5′–3′ exonuclease activity

required for cytoplasmic mRNA turn-over (Gel III). This is consistent with reports showing that the absence of Xrn1 stabilized mRNAs, which were decapped and maintained residual 10 to 15 As following deadenylation (Muhlrad et al. 1994). Other mutants with short A-tracts included Δ*sac3*, Δ*yke2* (Gel I), Δ*vps33*, Δ*ies3* (Gel III), and Δ*rad6*, Δ*ada2*, Δ*rpl21a*, Δ*swc1* (Gel IV). Intermediate poly(A) tracts were observed in the Δ*vps34* mutant (Gel II). Vps34 is a phosphatidylinositol 3-kinase that forms a complex with

FIGURE 6. Cordycepin-responsive mutants are linked to poly(A) metabolism. (*A*) Mutations causing cordycepin sensitivity genetically interact with *rna14-1*. The temperature-sensitive *rna14-1* strain, carrying a *URA3*-marked plasmid containing the wild-type *RNA14* gene, was used for disruption of genes causing cordycepin sensitivity. Double mutants were challenged with 5-flouroorotic acid (5-FOA) to force loss of the *URA3*-marked plasmid exhibiting the phenotype of the double mutation. Shown are serial dilutions of indicated single and double mutant strains on synthetic (SD) medium lacking or containing 5-FOA. Growth phenotypes were categorized as synthetic lethal (no growth), synthetic sick (reduced growth), or normal (no phenotype) when compared to the *rna14-1* mutant alone. (*B*) Cellular poly(A) length distribution in cordycepin-responsive strains. Total RNA was obtained from indicated mutant strains and analyzed as described in the legend of Figure 2A, except that poly(A) tails were resolved on 10% sequencing gels.

Vps15 (Stack et al. 1993); interestingly, the $\Delta vps15$ mutant was also identified in our screening and also displayed aberrant poly(A) length distribution (Gel III). These observations suggested a role for the Vps34–Vps15 complex or the signaling molecule phosphatidylinositol 3-phosphate, respectively, in poly(A) metabolism. Other mutants that had accumulated A-tracts of intermediate length included $\Delta pep5$, $\Delta thp1$ (Gel I), $\Delta bud32$ (Gel III), and $\Delta yor331c$ (Gel IV). The $\Delta reg1$ strain accumulated long poly(A) tails (Gel IV). Interestingly, Reg1 is a regulatory subunit for the type-1 protein phosphatase Glc7p that is involved in glucose repression (Tu and Carlson 1995). The poly(A) phenotype observed here may reflect a previously described role for Reg1 in controlling mRNA translation in response to nutrient status (Ashe et al. 2000) and may point to a requirement for Reg1-Glc7 in the maintenance of poly(A) tail length homeostasis.

DISCUSSION

We present a comprehensive study of the effects of cordycepin in the yeast *S. cerevisiae* that was initiated to increase the understanding of the molecular modes of action of this drug, on the one hand, and, on the other hand, to exploit its properties for the identification of novel genes that are functionally connected to poly(A) metabolism.

It is well established that cordycepin can terminate RNA synthesis when incorporated by RNA polymerases and poly(A) polymerase (Horowitz et al. 1976; Muller et al. 1977). While this conclusion is supported strongly by in vitro experiments, the effects of the drug in vivo remained less well characterized. Consistent with previous reports (Lecoq et al. 2001; Naula et al. 2003), our analyses support the idea that CoTP rather than cordycepin is mediating the toxicity of the drug in yeast. Since CoTP is an analog of ATP, this nucleotide may interfere with numerous cellular processes that require ATP binding or hydrolysis. While this remains a viable possibility, our analysis of suppressors of cordycepin toxicity identified mutants in three major activities: (1) nucleotide synthesis pathways that are involved in the conversion of cordycepin to CoTP; (2) poly(A) polymerase; and (3) cytoplasmic mRNA turn-over reactions. The latter observation suggested that mRNA stabilization suppressed toxicity, supporting the idea that it is, indeed, the inhibition of RNA synthesis that was limiting cell growth. Consistently, we observed strongly reduced steady-state mRNA levels following cordycepin treatment. This reduction of mRNA levels may result from the inhibition of transcript synthesis by RNA polymerase II, the abortion of poly(A) addition by poly(A) polymerase, or the inhibition of other reactions that are necessary for stable mRNA accumulation.

Unexpectedly, we observed cordycepin mediated phenotypes that cannot be explained by the RNA chain termination potential of the drug. Particularly striking were rapid effects on the 3′ ends of *ACT1* and *ASC1* mRNAs. For *ACT1*, it was suggested that a cluster of alternative poly(A) sites guides 3′ end formation and that the efficiency of poly(A) site recognition may determine the relative usage of these sites (Mandart and Parker 1995). Consistent with this idea, several mutants in 3′ end factors interfered with *ACT1* 3′ ends (Mandart and Parker 1995; Dichtl et al. 2002b; Kyburz et al. 2003). The duplication of these phenotypes by cordycepin in the wild type was unexpected since the preferred usage of site I was shifted to the more distal site V, resulting in longer transcripts (Fig. 2C). Since shorter RNAs would be predicted to result from chain termination, we conclude that the defect at *ACT1* did not result from cordycepin-induced termination of RNA polymerase II transcription. The accumulation of mRNAs with more distal 3′ ends also argued against chain termination during poly(A) synthesis by Pap1. The latter conclusion was furthermore underscored by the positive effect that cordycepin had on growth of *pap1* mutants (see below). Indeed, it was maybe one of the most surprising results of this study that the drug did not enhance the growth defect of *pap1* mutants. Since the *ACT1* defect was observed only minutes following exposure of the yeasts to the drug, and since the phenotype was suppressed in $\Delta ado1$ cells, it was probably directly mediated by CoTP. We also observed heterogeneous 3′ ends for *ASC1* mRNA, and also in this case cordycepin treatment affected their relative abundance in favor of the more distal 3′ ends. Therefore, similar mechanisms may mediate the effects of cordycepin on 3′ end formation on *ACT1* and *ASC1*.

Another unexpected observation was the appearance of extended *CYH2* mRNAs in the presence of cordycepin. Transcripts with discrete length appeared within minutes of drug addition and extended several kilobases beyond the normal 3′ end of the pre-mRNA, strongly suggesting that RNA chain termination was not the major consequence of cordycepin treatment. Instead, cordycepin apparently interfered with efficient 3′ end formation at the *CYH2* poly(A) site as was observed with *ACT1* and *ASC1* mRNAs. In contrast to the latter transcripts, which harbor clusters of poly(A) sites in their 3′ UTR, extended *CYH2* RNAs may result from 3′ end formation at the next available poly(A) sites, which lie far downstream from the regular site. How cordycepin reduces 3′ end formation efficiency remains unclear, but involved pathways may include the coupling of 3′ end formation to transcription (Lykke-Andersen and Jensen 2007). Consistent with this idea, we found that mutations in kinases and phosphatases that act on the CTD are hypersensitive to cordycepin (Fig. 1A).

Furthermore, our gene expression profiling experiments revealed that cordycepin treatment caused an increase of transcripts that were derived from dubious ORFs. This included the well-studied CUT *NEL025c*, which is degraded by exosome and TRAMP mediated mechanisms (Wyers et al. 2005; Houseley et al. 2006). A satisfying explanation for

the observed effects on *NEL025c* could be that TRAMP mediated polyadenylation was inhibited following cordycepin incorporation causing less efficient turn-over of the RNA. Alternatively, it seems possible that exosome-mediated degradation was impaired when the substrate RNA lacked a 3′ hydroxyl moiety. However, the major effect of cordycepin on *NEL025c* expression was the appearance of extended transcripts, which were likely to result from 3′ end formation at sites downstream from the Nrd1-dependent terminator that normally guides 3′ end formation of this transcript (Fig. 3E; Arigo et al. 2006; Thiebaut et al. 2006). Downstream termination on this transcription unit has been shown to include a Pap1 dependent site, providing another possible explanation for the accumulation of these and other RNAs in the presence of the drug. Since the Nrd1 complex is targeted to transcription units by serine 5 phosphorylated CTD (Gudipati et al. 2008; Vasiljeva et al. 2008), it is tempting to speculate that cordycepin treatment reduced the coupling of 3′ end formation to transcription also at *NEL025c*, as we suggested above for *ACT1*, *ASC1*, and *CYH2* mRNAs.

Overall, our data support the idea that the observed biochemical effects of cordycepin occurred largely independently from RNA chain termination. This unexpected conclusion may indicate that the nuclear concentration of CoTP that built up under the conditions employed here was sufficiently high to reduce the efficiency of 3′ end formation, but too low to cause significant chain termination either during transcription or polyadenylation. It will be interesting to test whether the same conclusion may apply to other organisms, be it prokaryotes or metazoans. However, our work implies that the impact of cordycepin on RNA synthesis has to be interpreted with caution and that it cannot generally be reduced to the chain termination potential of the drug. While the target of cordycepin action remains to be identified, the ameliorating effects of cordycepin on growth of *pap1* mutants (Fig. 1B) suggested an epistatic relationship between polyadenylation and cordycepin action. Such an epistatic effect is consistent with the idea that mutation of poly(A) polymerase and the presence of cordycepin interfere with the same pathway (Schuldiner et al. 2005; Segre et al. 2005).

Moreover, our analyses revealed that inactivation of poly(A) polymerase provoked higher cellular ATP levels in temperature-sensitive mutant strains. Our data are also consistent with the idea that the CoTP:ATP ratio is an important determinant for cordycepin toxicity, providing a plausible explanation of how poly(A) polymerase mutants suppressed cordycepin toxicity. Interestingly, a recent report revealed an ATP-sensing mechanism to connect RNA abundance to respiration (Amiott and Jaehning 2006). Our results suggest a reverse flow of information and raise the interesting possibility that the "efficiency" of gene expression (in this case, of polyadenylation) is somehow sensed and functionally linked to the energy status of the cell. However, further analyses are required to untangle this intriguing interplay of ATP homeostasis and 3′ end formation.

One of our motivations to analyze the effects of cordycepin was to establish a correlation of drug mediated phenotypes and functional classes of genes. Direct analysis of mutants involved in RNA synthesis and turn-over pathways clearly established cordycepin-responsive phenotypes. Our screening approaches using the deletion collection of non-essential genes identified genome-wide targets for the drug, and only a rather limited number of those genes is known to be involved in RNA synthesis and processing. This may reflect that genes involved in those processes often are essential for cell viability and were therefore not represented in the mutant collection that we screened. Nevertheless, we were able to link several functional categories of mutants with high significance to cordycepin action. This included chromatin associated proteins like the SAGA and SWR1 complexes, but the molecular reasons for cordycepin-responsive growth of the respective mutants remain to be determined.

Our analyses demonstrated that cordycepin meditated growth phenotypes can be useful indicators to identify genes that are involved in poly(A) metabolism. Several mutant strains were identified that showed aberrant poly(A) length distribution profiles (Fig. 6B). While the mechanistic relation of cordycepin-responsive growth and poly(A) distribution remains unclear for certain mutants, we can rationalize the situation in some cases. For example, Δ*xrn1* strains stabilize decapped mRNAs that retain residual short poly(A) tails (Muhlrad et al. 1994). The apparent accumulation of short poly(A) tracts can therefore reflect defective mRNA turn-over, which we found to suppress the toxic inhibition of RNA synthesis by cordycepin (Fig. 1C). In addition to mRNA turn-over enzymes, translation efficiency is thought to affect mRNA stability (Meyer et al. 2004). In cordycepin-hypersensitive Δ*reg1* strains, the accumulation of long poly(A) tracts may reflect a synergism between deregulated translation (Ashe et al. 2000) and reduced mRNA synthesis in the presence of cordycepin. Other cordycepin phenotypes may have resulted from enhancement of nuclear deficiencies that have an impact on poly(A) metabolism. For example, Thp1 and Sac3 form a nuclear-pore-associated complex that is required for efficient mRNA export (Fischer et al. 2002). Nuclear poly(A) accumulation may underlie the disturbed poly(A) profiles observed here in Δ*thp1* and Δ*sac3* strains, and less efficient gene expression in these strains likely synergized with the toxic effects of cordycepin. Moreover, it seems possible that loss of control of adenylation or deadenylation activities may contribute to poly(A) tail phenotypes in certain mutants. Non-essential components involved in poly(A) metabolism may primarily be involved in fine-tuning and regulatory aspects of gene expression. In this respect, it will be interesting to test, for example, which role

signal-transduction pathways and signaling molecules like the Vps34/Vps15 and its product phosphatidylinositol 3-phosphate play in the control of global poly(A) levels during growth and development or in response to changing environmental conditions. It seems likely that these and other cordycepin-responsive pathways identified in this work may help to uncover novel regulatory layers of poly(A) metabolism.

MATERIALS AND METHODS

Growth and construction of yeast strains

The *S. cerevisiae* strains used in this study are listed in Table 1. Yeast were grown in rich YPD medium (2% glucose, 2% bacto-tryptone, 1% yeast extract) or synthetic complete or synthetic drop-out media (2% glucose, 0.67% yeast nitrogen base, 1× amino acids). Cordycepin (Sigma-Aldrich) was supplemented at a concentration of 20 μg/mL unless stated otherwise. For synthetic interaction analyses, *kanMX4*-marked alleles were amplified from haploid mutant strains (Winzeler et al. 1999) and transferred into the *rna14-1* mutant background. Loss of *URA3*-marked plasmids was forced on SD plates containing 1 mg/mL 5-FOA (Zymo Research).

Drug sensitivity screening

For drop-test screening, all haploid mutants of the yeast gene deletion collection (Euroscarf) (Winzeler et al. 1999) were grown in 96-well microtiter plates and spotted on agar plates as single drops. Growth was examined daily for a 5-d period by comparing the drops on SD and SD cordycepin (20 μg/mL; Sigma-Aldrich) medium. Candidate strains were re-examined in two consecutive rounds by analyzing growth of 10-fold serial dilutions on SD supplemented with 40 μg/mL and 20 μg/mL cordycepin, respectively. The verified strains were then categorized as strong, medium, and weakly responsive to cordycepin, reflecting the relative confidence in the observed phenotype (Supplemental Data S1).

Chemical-genetic profiling was done essentially as described (Decourty et al. 2008). All haploid mutants of the yeast gene

deletion collection were pooled and cultured overnight in SD medium at 30°C. At an OD_{600} of 1.0, the culture was diluted 20-fold in SD medium lacking and containing 20 μg/mL cordycepin, respectively, and the OD_{600} was monitored every hour. After zero, 12, and 18 generations, 10 mL of cell culture was harvested. Genomic DNA extraction, labeling of the probes, hybridization to arrays, and analysis of the data was done as described (Decourty et al. 2008). Data are available in Supplemental Data S2.

RNA analyses

RNA extractions were done with a hot-phenol method as previously described (Holbein et al. 2008). Northern blot analysis was done with RNAs resolved either on 1.2% denaturing formaldeyde/agarose gels or with high-resolution 6% polyacrylamide/8.3 M urea gels (Dichtl et al. 2002b). *ASC1*, *ACT1*, *ADH1*, *PGK1*, and *CYH2* mRNAs were detected with ^{32}P random prime labeled PCR products (primer sequences are available upon request) corresponding to parts of the open reading frames. For *CYH2*, a PCR product was also used that encompassed intronic sequences; the CUT NEL025c was detected with a labeled PCR product amplified with forward GATTAACAGTTAGATCCAG and reverse GGACTT TCAGATCAGTCAGTG primers. 18S rRNA (ACGAAAAATCAA ATAC), U3 snoRNA (AGGACATTTCTATAGGAATCG), and $tRNA_3^{LEU}$ (GAACTCTTGCATCTTACGATAGC) were detected with 5′ end labeled oligonucleotides. RNase H analyses (Dichtl et al. 2002b) and poly(A) tail labeling (Holbein et al. 2008) were done as previously described. Northern filters and dried gels were exposed to BAS-MS imaging plates (Fuji) and developed on a FLA-7000 PhosphorImager (Fuji).

ATP measurements

ATP quantification was done as described (Freimoser et al. 2006). One OD_{600} equivalent of yeast cells was pelleted, the supernatant was discarded, 50 μL of 1 M sulfuric acid were added, and the suspension was neutralized with 50 μL of 2 M NaOH and 100 μL of Tris-malate buffer (1 M, pH 7.5, 6% neutral red solution [0.1% neutral red in 70% ethanol]). Cell debris was pelleted by centrifugation, 20 μL of the supernatant was added to 80 μL of Tris buffer (20 mM at pH 8, 2 mM EDTA), and 4 μL of phosphoenol pyruvate were added (2.5 mM PEP at pH 8, 0.125 M $MgSO_4$, 0.312 M K_2SO_4). Five microliters of this sample were

TABLE 1. Yeast strains used in this study

Strain	Genotype	Source/reference
kin28-ts3	*Mat a; leu2; trp1; ura3; ade2; ade3; lys2; kin28-ts3*	Valay et al. (1995)
pap1-1	*Mat a; ade1/ade2; lys2; gal? ; Ura3-52; pap1-1*	Patel and Butler (1992)
pap1-2	*Mat α; pap1::LEU2; pA-pap1-2-TRP1; ura3-1; his3-11*	Walter Keller[a]
pap1-5	*Mat α; pap1::LEU2; pA-pap1-5-TRP1; ura3-1; his3-11*	Walter Keller[a]
pap1-7	*Mat α; pap1::LEU2; pA-pap1-7-TRP1; ura3-1; his3-11*	Walter Keller[a]
rat1-1	*Mat a; ura3-52; leu2Δ1; hisΔ200; rat1-1*	Amberg et al. (1992)
rna14-1	*Mat a; ura3-1; trp1-1; ade2-1; leu2-3; 112; his3-11; 15; rna14-1*	Minvielle-Sebastia et al. (1994)
rna15-1	*Mat a; ura3-1; trp1-1; ade2-1; leu2-3; 112; his3-11; 15; rna15-1*	Minvielle-Sebastia et al. (1994)
rpb1-1	*Mat a; ura3-52; rpb1-1*	Nonet et al. (1987)
S288C	*MATα; SUC2; gal2; mal; mel; flo1; flo8-1; hap1; ho; bio1; bio6*	Mortimer and Johnson (1986)
ssu72-2	*Mat a; ura3-1; trp1-1; ade2-1; leu2-3; 112; his3-11; 15; ssu72-2*	Dichtl et al. (2002a)
ysh1-3	*Mat a; ura3-1; trp1-1; ade2-1; leu2-3; his3-11; 15; TRP1::ysh1 [ysh1-3-HIS3-CEN]*	Garas et al. (2008)

[a]Gift (Biozentrum, University of Basel).

added to 45 μL of luciferase buffer (10 mM Tris-H_2SO_4 at pH 7.4, 3.5 mM $MgSO_4$). Following addition of 50 μL of luciferase solution (Roche ATP Bioluminescence Assay kit CLS II), relative light units emitted were measured in a luminometer (Lumat LB 9507; Berthold Technologies).

Microarray analyses

Wild-type S228C and *pap1-1* were grown in SD medium at 25°C to OD_{600} 0.3, and growth was continued for 1 h in the presence or absence of 20 μg/mL cordycepin. All subsequent steps will be described elsewhere (Halbeisen and Gerber 2009). Shortly, RNA was extracted from cell pellets using a hot-phenol method and further purification with the RNeasy Micro Kit (QIAGEN). Ten micrograms of total RNA were used for reverse transcription using superscript II (Invitrogen) with oligo(dT) and pdN9 primers and Ambion spike control. Following RNA hydrolysis and neutralization, DNA was concentrated to 9 μL using the Microcon-30 concentrator (Amicon). NHS-Cy3 and NHS-Cy5 dyes (Amersham) were coupled to the DNA and purified using the Qia-quick PCR purification kit (QIAGEN). The Cy3- and Cy5-labeled cDNA samples were mixed and concentrated in Microcon-30 concentrators (Amicon) to a final volume of 10.5 μL, and labeling efficiency was measured by NanoDrop using the microarray application.

The concentrated labeled DNA was mixed with MWG formamide buffer (Ocimun Biosolutions), and poly(A) RNA was added to a final concentration of 0.5 mg/mL. The mix was incubated for 10 min at 80°C, loaded on Nexterion slides (carrying 70-mer oligo probes for 10,944 features), and hybridized overnight at 42°C. Following washes in 2× SSC, 0.2% SDS and 2× SSC, and 0.2× SSC, the arrays were immersed in 100% ethanol to fix the cDNA, dried by centrifugation, and scanned with Axon instruments scanner 4000. Scanning parameters were adjusted to similar fluorescent intensities in both channels, and data were collected with GENEPIX 3.0 (Axon Instruments). Spots with abnormal morphology were identified by eye and excluded from further analysis. Arrays were normalized by the Stanford Microarray Database (SMD) (Gollub et al. 2003). The calculated log_2 ratios were imported into Acuity 4.0 (Axon Instruments) and filtered for regression correlation of >0.5 (filters for large variations in the ratios of pixels within each spot) and a signal-to-noise ratio of >2.5 (signal over background). Average log_2 ratios were calculated from the triple experiments for each gene spot. RNAs were considered as increased when the log_2 ratio was >1 and decreased when log_2 was <−1. Further analysis of the data was carried out with the *Saccharomyces* Genome Database GO term finder (http://www.yeastgenome.org/). Microarray data were deposited at GEO (http://www.ncbi.nlm.nih.gov/geo; GEO accession: GSE14619), and processed data are also available as Supplemental Data S3.

SUPPLEMENTAL MATERIAL

Supplemental material can be found at http://www.rnajournal.org.

ACKNOWLEDGMENTS

REFERENCES

Ahn, Y.J., Park, S.J., Lee, S.G., Shin, S.C., and Choi, D.H. 2000. Cordycepin: Selective growth inhibitor derived from liquid culture of *Cordyceps militaris* against *Clostridium* spp. *J. Agric. Food Chem.* **48:** 2744–2748.

Amberg, D.C., Goldstein, A.L., and Cole, C.N. 1992. Isolation and characterization of *RAT1*: An essential gene of *Saccharomyces cerevisiae* required for the efficient nucleocytoplasmic trafficking of mRNA. *Genes & Dev.* **6:** 1173–1189.

Amiott, E.A. and Jaehning, J.A. 2006. Mitochondrial transcription is regulated via an ATP ''sensing'' mechanism that couples RNA abundance to respiration. *Mol. Cell* **22:** 329–338.

Arigo, J.T., Eyler, D.E., Carroll, K.L., and Corden, J.L. 2006. Termination of cryptic unstable transcripts is directed by yeast RNA-binding proteins Nrd1 and Nab3. *Mol. Cell* **23:** 841–851.

Ashe, M.P., De Long, S.K., and Sachs, A.B. 2000. Glucose depletion rapidly inhibits translation initiation in yeast. *Mol. Biol. Cell* **11:** 833–848.

Bloch, J.C., Perrin, F., and Lacroute, F. 1978. Yeast temperature-sensitive mutants specifically impaired in processing of poly(A)-containing RNAs. *Mol. Gen. Genet.* **165:** 123–127.

Boeck, R., Tarun Jr., S., Rieger, M., Deardorff, J.A., Muller-Auer, S., and Sachs, A.B. 1996. The yeast Pan2 protein is required for poly(A)-binding protein-stimulated poly(A)-nuclease activity. *J. Biol. Chem.* **271:** 432–438.

Brown, C.E. and Sachs, A.B. 1998. Poly(A) tail length control in *Saccharomyces cerevisiae* occurs by message-specific deadenylation. *Mol. Cell. Biol.* **18:** 6548–6559.

Brown, C.E., Tarun Jr., S.Z., Boeck, R., and Sachs, A.B. 1996. *PAN3* encodes a subunit of the Pab1p-dependent poly(A) nuclease in *Saccharomyces cerevisiae*. *Mol. Cell. Biol.* **16:** 5744–5753.

Brown, J.T., Bai, X., and Johnson, A.W. 2000. The yeast antiviral proteins Ski2p, Ski3p, and Ski8p exist as a complex in vivo. *RNA* **6:** 449–457.

Cunningham, K.G., Manson, W., Spring, F.S., and Hutchinson, S.A. 1950. Cordycepin, a metabolic product isolated from cultures of *Cordyceps militaris* (Linn.) Link. *Nature* **166:** 949.

Daugeron, M.C., Mauxion, F., and Seraphin, B. 2001. The yeast *POP2* gene encodes a nuclease involved in mRNA deadenylation. *Nucleic Acids Res.* **29:** 2448–2455.

Decourty, L., Saveanu, C., Zemam, K., Hantraye, F., Frachon, E., Rousselle, J.C., Fromont-Racine, M., and Jacquier, A. 2008. Linking functionally related genes by sensitive and quantitative characterization of genetic interaction profiles. *Proc. Natl. Acad. Sci.* **105:** 5821–5826.

Desmoucelles, C., Pinson, B., Saint-Marc, C., and Daignan-Fornier, B. 2002. Screening the yeast ''disruptome'' for mutants affecting resistance to the immunosuppressive drug, mycophenolic acid. *J. Biol. Chem.* **277:** 27036–27044.

Dichtl, B., Blank, D., Ohnacker, M., Friedlein, A., Roeder, D., Langen, H., and Keller, W. 2002a. A role for *SSU72* in balancing RNA polymerase II transcription elongation and termination. *Mol. Cell* **10:** 1139–1150.

Dichtl, B., Blank, D., Sadowski, M., Hubner, W., Weiser, S., and Keller, W. 2002b. Yhh1p/Cft1p directly links poly(A) site recognition

and RNA polymerase II transcription termination. *EMBO J.* **21:** 4125–4135.

Fischer, T., Strasser, K., Racz, A., Rodriguez-Navarro, S., Oppizzi, M., Ihrig, P., Lechner, J., and Hurt, E. 2002. The mRNA export machinery requires the novel Sac3p–Thp1p complex to dock at the nucleoplasmic entrance of the nuclear pores. *EMBO J.* **21:** 5843–5852.

Freimoser, F.M., Hurlimann, H.C., Jakob, C.A., Werner, T.P., and Amrhein, N. 2006. Systematic screening of polyphosphate (poly P) levels in yeast mutant cells reveals strong interdependence with primary metabolism. *Genome Biol.* **7:** R109. doi: 10.1186/gb-2006-7-11-r109.

Garas, M., Dichtl, B., and Keller, W. 2008. The role of the putative 3′ end processing endonuclease Ysh1p in mRNA and snoRNA synthesis. *RNA* **14:** 2671–2684.

Gollub, J., Ball, C.A., Binkley, G., Demeter, J., Finkelstein, D.B., Hebert, J.M., Hernandez-Boussard, T., Jin, H., Kaloper, M., Matese, J.C., et al. 2003. The Stanford Microarray Database: Data access and quality assessment tools. *Nucleic Acids Res.* **31:** 94–96.

Gudipati, R.K., Villa, T., Boulay, J., and Libri, D. 2008. Phosphorylation of the RNA polymerase II C-terminal domain dictates transcription termination choice. *Nat. Struct. Mol. Biol.* **15:** 786–794.

Halbeisen, R.E. and Gerber, A.P. 2009. Stress-dependent coordination of transcriptome and translatome in yeast. *PLoS Biol.* (in press).

Hillenmeyer, M.E., Fung, E., Wildenhain, J., Pierce, S.E., Hoon, S., Lee, W., Proctor, M., St Onge, R.P., Tyers, M., Koller, D., et al. 2008. The chemical genomic portrait of yeast: Uncovering a phenotype for all genes. *Science* **320:** 362–365.

Hilleren, P. and Parker, R. 2001. Defects in the mRNA export factors Rat7p, Gle1p, Mex67p, and Rat8p cause hyperadenylation during 3′ end formation of nascent transcripts. *RNA* **7:** 753–764.

Holbein, S., Freimoser, F.M., Werner, T.P., Wengi, A., and Dichtl, B. 2008. Cordycepin-hypersensitive growth links elevated polyphosphate levels to inhibition of poly(A) polymerase in *Saccharomyces cerevisiae. Nucleic Acids Res.* **36:** 353–363.

Horowitz, B., Goldfinger, B.A., and Marmur, J. 1976. Effect of cordycepin triphosphate on the nuclear DNA-dependent RNA polymerases and poly(A) polymerase from the yeast, *Saccharomyces cerevisiae. Arch. Biochem. Biophys.* **172:** 143–148.

Houseley, J., LaCava, J., and Tollervey, D. 2006. RNA-quality control by the exosome. *Nat. Rev. Mol. Cell Biol.* **7:** 529–539.

Kiel, J.A., Veenhuis, M., and van der Klei, I.J. 2006. PEX genes in fungal genomes: Common, rare or redundant. *Traffic* **7:** 1291–1303.

Konrad, M. 1988. Analysis and in vivo disruption of the gene coding for adenylate kinase (*ADK1*) in the yeast *Saccharomyces cerevisiae. J. Biol. Chem.* **263:** 19468–19474.

Kyburz, A., Sadowski, M., Dichtl, B., and Keller, W. 2003. The role of the yeast cleavage and polyadenylation factor subunit Ydh1p/Cft2p in pre-mRNA 3′ end formation. *Nucleic Acids Res.* **31:** 3936–3945.

Lecoq, K., Belloc, I., Desgranges, C., and Daignan-Fornier, B. 2001. Role of adenosine kinase in *Saccharomyces cerevisiae*: Identification of the *ADO1* gene and study of the mutant phenotypes. *Yeast* **18:** 335–342.

Lykke-Andersen, S. and Jensen, T.H. 2007. Overlapping pathways dictate termination of RNA polymerase II transcription. *Biochimie* **89:** 1177–1182.

Mandart, E. and Parker, R. 1995. Effects of mutations in the *Saccharomyces cerevisiae RNA14, RNA15*, and *PAP1* genes on polyadenylation in vivo. *Mol. Cell. Biol.* **15:** 6979–6986.

Maser, P., Sutterlin, C., Kralli, A., and Kaminsky, R. 1999. A nucleoside transporter from *Trypanosoma brucei* involved in drug resistance. *Science* **285:** 242–244.

Meyer, S., Temme, C., and Wahle, E. 2004. Messenger RNA turnover in eukaryotes: Pathways and enzymes. *Crit. Rev. Biochem. Mol. Biol.* **39:** 197–216.

Minvielle-Sebastia, L., Preker, P.J., and Keller, W. 1994. *RNA14* and *RNA15* proteins as components of a yeast pre-mRNA 3′ end processing factor. *Science* **266:** 1702–1705.

Mortimer, R.K. and Johnston, J.R. 1986. Genealogy of principal strains of the yeast genetic stock center. *Genetics* **113:** 35–43.

Muhlrad, D., Decker, C.J., and Parker, R. 1994. Deadenylation of the unstable mRNA encoded by the yeast *MFA2* gene leads to decapping followed by 5′ → 3′ digestion of the transcript. *Genes & Dev.* **8:** 855–866.

Muller, W.E., Seibert, G., Beyer, R., Breter, H.J., Maidhof, A., and Zahn, R.K. 1977. Effect of cordycepin on nucleic acid metabolism in L5178Y cells and on nucleic acid-synthesizing enzyme systems. *Cancer Res.* **37:** 3824–3833.

Naula, N., Hilti, N., Schweingruber, A.M., and Schweingruber, M.E. 2003. Cordycepin in *Schizosaccharomyces pombe*: Effects on the wild type and phenotypes of mutants resistant to the drug. *Curr. Genet.* **43:** 400–406.

Nonet, M., Scafe, C., Sexton, J., and Young, R. 1987. Eukaryotic RNA polymerase conditional mutant that rapidly ceases mRNA synthesis. *Mol. Cell. Biol.* **7:** 1602–1611.

Ooi, S.L., Pan, X., Peyser, B.D., Ye, P., Meluh, P.B., Yuan, D.S., Irizarry, R.A., Bader, J.S., Spencer, F.A., and Boeke, J.D. 2006. Global synthetic-lethality analysis and yeast functional profiling. *Trends Genet.* **22:** 56–63.

Parsons, A.B., Lopez, A., Givoni, I.E., Williams, D.E., Gray, C.A., Porter, J., Chua, G., Sopko, R., Brost, R.L., Ho, C.H., et al. 2006. Exploring the mode-of-action of bioactive compounds by chemical-genetic profiling in yeast. *Cell* **126:** 611–625.

Patel, D. and Butler, J.S. 1992. Conditional defect in mRNA 3′ end processing caused by a mutation in the gene for poly(A) polymerase. *Mol. Cell. Biol.* **12:** 3297–3304.

Paterson, R.R. 2008. Cordyceps: A traditional Chinese medicine and another fungal therapeutic biofactory? *Phytochemistry* **69:** 1469–1495.

Rottenberg, M.E., Masocha, W., Ferella, M., Petitto-Assis, F., Goto, H., Kristensson, K., McCaffrey, R., and Wigzell, H. 2005. Treatment of African trypanosomiasis with cordycepin and adenosine deaminase inhibitors in a mouse model. *J. Infect. Dis.* **192:** 1658–1665.

Schuldiner, M., Collins, S.R., Thompson, N.J., Denic, V., Bhamidipati, A., Punna, T., Ihmels, J., Andrews, B., Boone, C., Greenblatt, J.F., et al. 2005. Exploration of the function and organization of the yeast early secretory pathway through an epistatic miniarray profile. *Cell* **123:** 507–519.

Segre, D., Deluna, A., Church, G.M., and Kishony, R. 2005. Modular epistasis in yeast metabolism. *Nat. Genet.* **37:** 77–83.

Stack, J.H., Herman, P.K., Schu, P.V., and Emr, S.D. 1993. A membrane-associated complex containing the Vps15 protein kinase and the Vps34 PI 3-kinase is essential for protein sorting to the yeast lysosome-like vacuole. *EMBO J.* **12:** 2195–2204.

Sugar, A.M. and McCaffrey, R.P. 1998. Antifungal activity of 3′-deoxyadenosine (cordycepin). *Antimicrob. Agents Chemother.* **42:** 1424–1427.

Thiebaut, M., Kisseleva-Romanova, E., Rougemaille, M., Boulay, J., and Libri, D. 2006. Transcription termination and nuclear degradation of cryptic unstable transcripts: A role for the Nrd1–Nab3 pathway in genome surveillance. *Mol. Cell* **23:** 853–864.

Tu, J. and Carlson, M. 1995. *REG1* binds to protein phosphatase type 1 and regulates glucose repression in *Saccharomyces cerevisiae. EMBO J.* **14:** 5939–5946.

Tucker, M., Staples, R.R., Valencia-Sanchez, M.A., Muhlrad, D., and Parker, R. 2002. Ccr4p is the catalytic subunit of a Ccr4p/Pop2p/Notp mRNA deadenylase complex in *Saccharomyces cerevisiae. EMBO J.* **21:** 1427–1436.

Valay, J.G., Simon, M., Dubois, M.F., Bensaude, O., Facca, C., and Faye, G. 1995. The *KIN28* gene is required both for RNA polymerase II mediated transcription and phosphorylation of the Rpb1p CTD. *J. Mol. Biol.* **249:** 535–544.

Vasiljeva, L., Kim, M., Mutschler, H., Buratowski, S., and Meinhart, A. 2008. The Nrd1–Nab3–Sen1 termination complex interacts with the Ser5-phosphorylated RNA polymerase II C-terminal domain. *Nat. Struct. Mol. Biol.* **15:** 795–804.

Wanders, R.J. and Waterham, H.R. 2006. Biochemistry of mammalian peroxisomes revisited. *Annu. Rev. Biochem.* **75:** 295–332.

Winzeler, E.A., Shoemaker, D.D., Astromoff, A., Liang, H., Anderson, K., Andre, B., Bangham, R., Benito, R., Boeke, J.D., Bussey, H., et al. 1999. Functional characterization of the *S. cerevisiae* genome by gene deletion and parallel analysis. *Science* **285:** 901–906.

Wyers, F., Rougemaille, M., Badis, G., Rousselle, J.C., Dufour, M.E., Boulay, J., Regnault, B., Devaux, F., Namane, A., Seraphin, B., et al. 2005. Cryptic Pol II transcripts are degraded by a nuclear quality control pathway involving a new poly(A) polymerase. *Cell* **121:** 725–737.

Zhu, J.S., Halpern, G.M., and Jones, K. 1998a. The scientific rediscovery of a precious ancient Chinese herbal regimen: *Cordyceps sinensis*: Part II. *J. Altern. Complement. Med.* **4:** 429–457.

Zhu, J.S., Halpern, G.M., and Jones, K. 1998b. The scientific rediscovery of an ancient Chinese herbal medicine: *Cordyceps sinensis*: part I. *J. Altern. Complement. Med.* **4:** 289–303.